Preferred Formation of Minority Concomitant Polymorphs in 2D Self-Assembly under Lateral Nanoconfinement

Johannes Seibel,[a] David B. Amabilino[b] and Steven De Feyter[a]*

Abstract: Control over polymorph formation in the crystallization of organic molecules remains a huge scientific challenge. Here, we present preferential formation of one polymorph, formed by chiral molecules, in controlled two-dimensional (2D) nanoconfinement conditions at a liquid/solid interface. So-called nanocorrals to control concomitant polymorph formation were created *in-situ* via a nanoshaving protocol at the interface between 1-phenyloctane and covalently modified highly-oriented pyrolytic graphite (HOPG). The preferentially formed polymorphs – that were less stable in the large-scale monolayers – could be selected simply by varying the orientation of the square nanocorrals with respect to the HOPG lattice.

Polymorphism is the ability of a given compound to form at least two different crystalline structures. While having the same chemical composition, each polymorph is unique with its own physical and chemical properties.[1] Due to these different properties, understanding and controlling polymorph formation of (chiral) organic compounds is of interest in pharmaceutical industries,[2,3] organic electronics and functional materials in general.[4,5] In particular in small-molecule organic semi-conductors (OSCs), the crystal structure often plays an important role in device performance. Consequently, numerous strategies to control morphology and polymorphism of OSCs in thin films have been developed.[6] Among the methods available nanoscale confinement has been proven to be an efficient way to achieve control over polymorph formation,[7] for example by using well-defined pores having dimensions in the order of the critical nucleation size.[8] Lateral confinement in a line-pattern has been shown to increase the crystallinity and lead to the alignment of crystalline domains of a small-molecule organic semiconductor using capillary force lithography[9] and in thin films prepared by solution shearing and partial de-wetting.[10] In molecular self-assembly at surfaces and interfaces[11] two-dimensional (2D) lateral nanoconfinement has been used to control the on-surface synthesis of organometallic chains and macrocycles.[12] Further, lateral nanoconfinement resulting from step-edges on atomically flat surfaces can affect polymorph formation of self-assembled molecular networks (SAMNs).[13,14]

[a] Dr. Johannes Seibel, Prof. Dr. Steven De Feyter
Department of Chemistry, Division of Molecular Imaging and Photonics,
KU Leuven – University of Leuven
Celestijnenlaan 200F, B-3001 Leuven, Belgium
E-mail: steven.defeyter@kuleuven.be
[b] Prof. Dr. David B. Amabilino
School of Chemistry & The GSK Carbon Neutral Laboratories for Sustainable Chemistry
The University of Nottingham
Triumph Road, Nottingham NG7 2TU, UK

Supporting information for this article is given via a link at the end of the document

However, these studies on lateral nanoconfinement of 2D SAMNs lack control over size and shape of the confinement conditions and the lateral confinement is static, as is the case in the OSCs confinement.

In this context, we have developed an *in-situ* nanoshaving protocol at the liquid/solid interface, which uses scanning tunneling microscopy (STM) as manipulation and visualization tool.[15] This approach allows the control over size and shape of the nanoconfinement and, in contrast to the studies mentioned, the size and shape of the confinement changes gradually, potentially giving additional insights into kinetics and thermodynamics of the 2D crystallization process.

To achieve this, highly-oriented pyrolytic graphite (HOPG) is covalently modified, *i.e.* grafted, with 3,5-bis-*tert*-butylphenyl (3,5-TBP) moieties using diazonium chemistry. A high-density of grafted molecules prevents physisorption and SAMN formation from a drop-cast solution. The grafted molecules can be removed again to restore the pristine HOPG surface in the presence of the drop-cast solution, enabling SAMN formation in well-defined areas, so-called nanocorrals (Figure 1c).

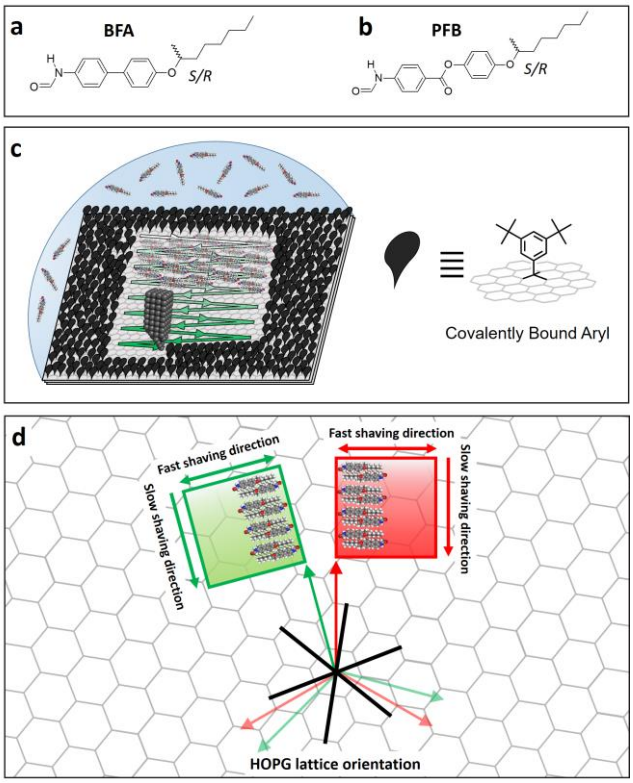

Figure 1. Structures of the molecules studied (a and b) and schematic representation of the *in-situ* nanoshaving process used to create nanocorrals for polymorph selection (c). Panel d shows the principle of polymorph selection using square-shaped nanocorrals with different orientations with respect to the HOPG lattice (not to scale). Rotational domains are indicated by arrows.

Using this approach, we have previously shown that lateral confinement and the *in-situ* nanoshaving process can have a significant impact on SAMN formation in nanocorrals.[16–19] Here, we control nanocorral orientation to induce a bias in the formation of concomitant polymorphs, which differ in their orientation with respect to the HOPG lattice. Their preferential formation could be achieved simply by varying the orientation of square-shaped nanocorrals with respect to the HOPG lattice (Figure 1). Further, we show how hydrogen bond (H-bond) directionality in combination with the *in-situ* nanoshaving process affects the molecular orientation and selection efficiency in the nanocorrals.

To achieve polymorph selection we chose molecules with a high aspect ratio, forming polymorphous structures having different angles with respect to the underlying HOPG lattice. Upon drop-casting a 10 mM solution of enantiopure 4-[(*S*/*R*-1-methylheptyl)oxy]-4'-biphenylformamide (*S*/*R*-BFA)[20] in 1-phenyloctane (PO) onto pristine HOPG, the molecules form an SAMN, appearing as a row-like structure in large-scale STM images (see supporting information S1 for experimental details) with two different orientations, taking into account the threefold symmetry of the surface (Figure 2a).

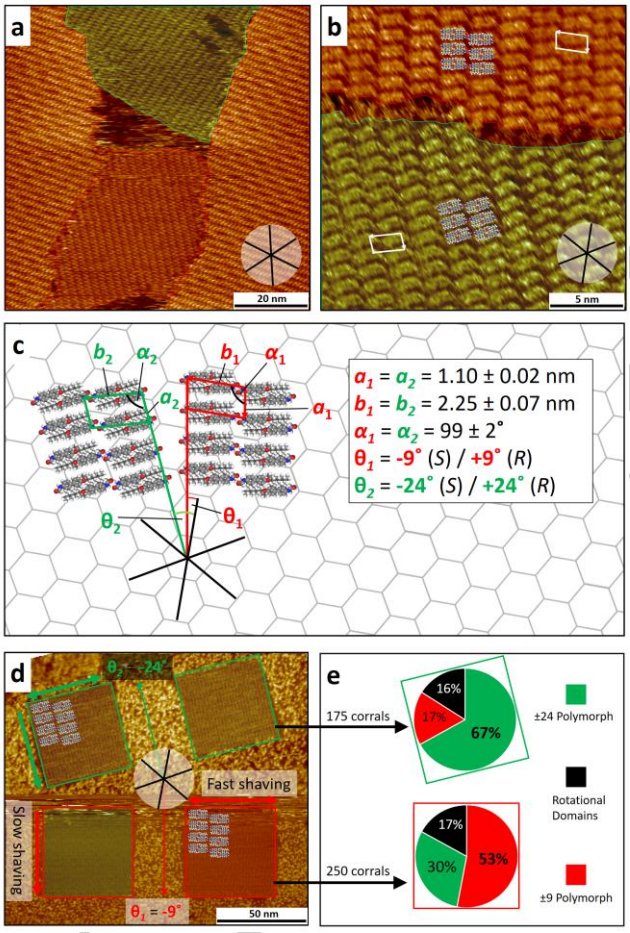

Figure 2. Large scale (a) and high-resolution (b) STM images of *S*-BFA at the pristine PO/HOPG interface at a concentration of 10 mM. Different polymorphs are colored red and green, respectively. The unit cell and molecular assembly for each polymorph is indicated in b. Panel c shows a tentative model for the assembly of *S*-BFA in relation to the HOPG lattice and the unit cell parameters for both enantiomers. *In-situ* created nanocorrals with angles of -9˚(bottom) and -24˚ (top) with respect to the HOPG lattice are shown in d. Molecular models indicate the assembly in relation to the nanocorral. Statistics of the polymorph distribution in the nanocorrals (e) show a clear bias towards the polymorph with the short unit cell vector parallel to the slow shaving direction. The black bar represents other rotational domains. Imaging parameters: I_t = 70 pA, V_b = -0.700 V.

High-resolution STM images reveal that these rows consist of head-to-tail dimers (Figure 2b). Imaging of the underlying HOPG lattice showed that the two different orientations have the same unit cell dimensions and only differ discernably in their orientation with respect to the HOPG lattice (Figure 2c). While we focus on one enantiomer in the following description of the obtained results, measurements were carried out with both enantiomers. The angles between the row-like features of the enantiomers and main symmetry axes of the HOPG lattice have opposite signs, *i.e.* +9˚ (θ_1) and +24˚ (θ_2) for *R*-BFA and -9˚ and -24˚ for *S*-BFA, respectively (Figure S1).

Square-shaped nanocorrals with the fast-shaving direction aligned along the long molecular axis of one of the polymorph structures, were used in the selection experiments. The row-like features, which are parallel to the short unit cell vector *a* and orthogonal to the long molecular axis, run parallel to the slow-shaving direction (Figure 2). Thereby, a bias in polymorph formation could be achieved simply by adjusting the nanocorral orientation (Figure 2e): Induction of the ±24˚ structure was more selective, which is the least favored polymorph in full monolayers on pristine HOPG (Figure S2). Note that while figures 2d and 3d are composed of two STM images for better illustration, the measurements were actually carried out with sets of four squares of the same orientation to minimize drift effects (Figure S3). In figure 2e the statistics are summarized for both enantiomers combined. More detailed statistics for each enantiomer are in the supporting information (Figure S4). Rotational domains were rarely observed and all corrals contained only a single domain.

The second molecule studied, enantiopure 4-[(*S*/*R*-1-methylheptyl)oxy]phenyl-4'-formamidobenzoate (*S*/*R*-PFB, figure 1b),[20,21] also forms row-like structures upon drop-casting a 5.5 mM solution in PO onto pristine HOPG with two different orientations (Figure 3 a and b). These rows either run in a ±30˚ angle (θ_2) with respect to a high-symmetry surface direction or are tilted with an angle (θ_1) of -22˚ (*R*-PFB) or +22˚ (*S*-PFB), respectively (Figure 3c and S1). Interestingly, adjacent polymorphs can merge without showing a clear domain boundary (Figure 3b). Similar to the BFA system, we first attempted the polymorph selection by creating squares with the long molecular axis aligned along the fast-shaving direction. However, this orientation did not result in any alignment of the rows parallel to the nanocorral side border (Figure S5). Thus, we attempted the selection of the polymorph with the short unit cell vector parallel to the top border (Figure 3d). Using this square orientation we were able to achieve polymorph selection, which showed a surprisingly high efficiency considering the difference of only 8˚ between the two polymorphs (Figure 3e). The statistics shown in figure 3e are summarized from measurement sessions with both enantiomers. Detailed statistics are shown in

the supporting information (Figure S6). More than one domain in a corral was rarely observed, but some corrals were only partially filled (Figure S7). Notably, the highest selection was achieved for the ±22 polymorph of the PFB system, which is the minority polymorph in the SAMN on pristine HOPG (Figure S2).

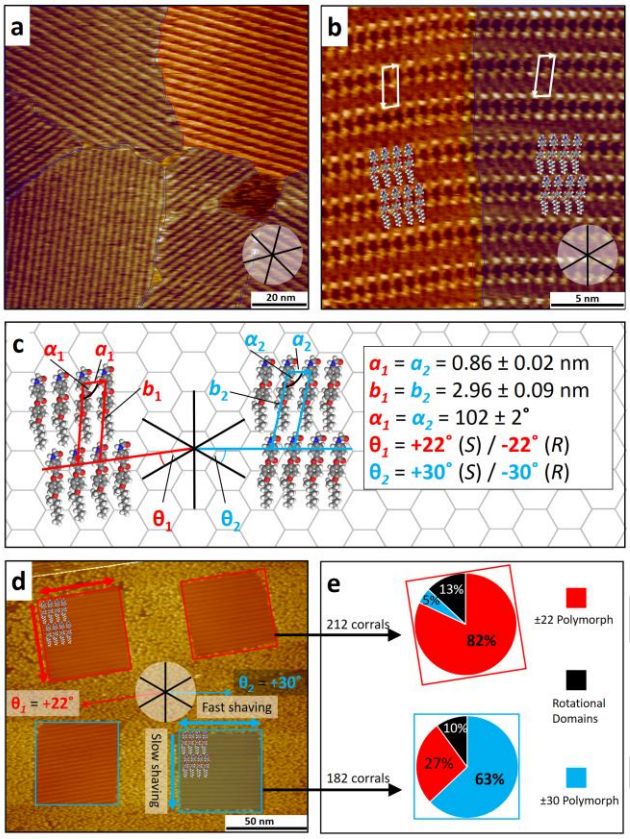

Figure 3. Large scale (a) and high-resolution (b) STM images of *S*-PFB at the pristine PO/HOPG interface at a concentration of 5.5 mM. Different polymorphs are colored red and blue. The unit cell and molecular assembly for each polymorph is indicated in b. Panel c shows a tentative model of the assembly of *S*-PFB in relation to the HOPG lattice and the unit cell parameters for both enantiomers. *In-situ* created nanocorrals with angles of +22˚(top) and +30˚ (bottom) with respect to the HOPG lattice are shown in d. Molecular models indicate the assembly in relation to the nanocorral. Statistics of the polymorph distribution in the nanocorrals (e) show a clear bias towards the polymorph with the row-structure parallel to the fast shaving direction. The black bar represents other rotational domains. Imaging parameters: I_t = 70 pA, V_b = -0.700 V.

Apart from the polymorph selection efficiency, the main difference between the two systems is the orientation of the row structure and long molecular axis in the selected domains. In the case of BFA, the long molecular axis is aligned along the fast-shaving direction and in contrast thereto, the PFB long molecular axis is aligned along the slow-shaving direction (Figure 4). Previously, we proposed that geometric constraints due to the long aspect ratio of the molecules in the initial stages of nanocorral formation play a major role in the observed domain selection.[16–18,22] This would, however, only explain the observed polymorph selection of the *R*/*S*-BFA system and is clearly not the case for the *R*/*S*-PFB system. This can be understood by looking at the directionality of possible intermolecular interactions in the confined 2D crystal structures (Figure 4). While BFA and PFB can both potentially form H-bonds via their formamide head-groups, the directionality of the intermolecular H-bonds in relation to the long molecular axis is significantly different. The BFA structure consists of head-to-tail dimers, which align in a straight line perpendicular to the long molecular axis (Figure 4a). This alignment allows H-bonding between the dimers, *i.e.* between adjacent rows, and van-der-Waals (vdW) interactions along the row structure. In contrast thereto, PFB assembles in rows of single molecules, resulting in intermolecular H-bonds and vdW interactions along the row structure (Figure 4b). Thus, in both molecular systems the intermolecular interactions are anisotropic and the H-bond direction is parallel to the fast shaving direction in the preferentially formed polymorphs.

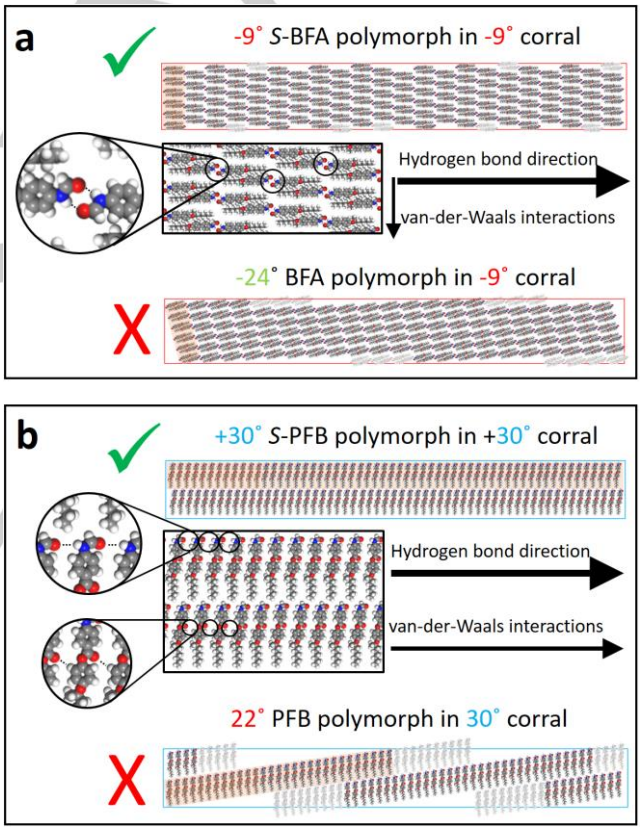

Figure 4. Tentative models of the molecular orientation of both polymorphs of BFA (a) and PFB (b), respectively, in the same nanocorral. The rectangular shape of the nanocorral is chosen to represent the shape during the initial stages of the nanoshaving process. Both of the preferentially-formed polymorphs have H-bond directionality along the fast-shaving direction. Additional vdW interactions are possible perpendicular to the H-bonds along the slow shaving direction in the BFA system and parallel to the H-bonds in the PFB system. In the case of BFA, the mismatching polymorph contains slightly less molecules and thus H-bonds (119 vs 113 dimers), while the difference between matching and mismatching polymorph of PFB is significantly higher (115 vs 75 molecules).

Due to the formation of single domains even in nanocorrals as large as 220 nm x 220 nm (Figure S8), we propose nucleation as the deciding step, *i.e.* the first polymorph that nucleates is the one growing as the nanocorral is being formed. Supporting this claim, we observed that *ex-situ* nanocorrals (created before drop-casting the solution) showed SAMNs formation with multiple domains and no alignment effects (Figure S9), highlighting the impact of the nanoshaving process on molecular self-assembly. That is, in the initial stages of nanocorral formation, when nucleation is expected to occur, the area available for molecular self-assembly has a rectangular shape and high aspect ratio, imposing geometrical constraints on the nucleus shape and thus stability, depending on the nucleus' orientation with respect to the nanocorral (Figure 4). Additionally, interactions between the SAMN and the nanocorral edges may affect the nucleus stability. A small high aspect ratio BFA nucleus of several adjacent short rows is thermodynamically favored due to a higher number of H-bonds, compared to fewer long rows (Figure S10) and the other polymorph (Figure 4a). Therefore, the former will be the first one to reach a critical stability on the surface under the given constraints. In contrast thereto, the intermolecular interactions in the PFB system are optimized by the formation of long rows rather than by several adjacent shorter rows (Figure S11). These long rows, however, can only form when they run exactly parallel to the top border of the nanocorral (Figure 4b). As a result, the selectivity in the PFB system is higher even though the angle between the two polymorphs is smaller compared to the BFA system. Furthermore, the higher selectivity in the nanocorrals of the minority polymorph suggests that it is kinetically preferred and may have a smaller critical nucleation size, while the other one is thermodynamically more stable. A further decrease in the relative appearance of the minority polymorphs on pristine HOPG after annealing supports this hypothesis (Figure S12).

In summary, we have presented preferential polymorph formation by enantiopure molecules at the liquid/solid interface using *in-situ* created nanocorrals. The polymorph selection solely depended on the orientation of the nanocorral with respect to the HOPG lattice, which can be chosen freely employing the nanoshaving protocol presented here. Anisotropic intermolecular interactions in the assembled structures are proposed to play a major role in the selection mechanism. We believe the domain selection with *in-situ* nanoshaving to be general phenomena in molecular systems with strong anisotropic intermolecular interactions that quickly nucleate, making this method a valuable tool to study molecular crystallization and nucleation at surfaces and interfaces. The potential of the method is proven by the fact that polymorphs that are the minority in large scale monolayers can be favored under nanoconfinement. Future work will involve racemic mixtures of the compounds studied here and their enantioselective adsorption in nanocorrals.

Acknowledgements

The authors gratefully acknowledge financial support from the Fund of Scientific Research Flanders (FWO), KU Leuven - Internal Funds, and FWO under EOS 30489208. J. S. acknowledges financial support through a Marie Skłodowska-Curie Individual Fellowship (EU project 789865 - EnSurf). D. B. A. thanks the EPSRC (project EP/M005178/1) and the School of Chemistry at the University of Nottingham for funding.

Keywords: 2D crystallization • Nanoconfinement • Polymorphism • Scanning Tunnelling Microscopy • Supramolecular Chemistry

[1] J. Bernstein, R. J. Davey, J.-O. Henck, *Angew. Chemie Int. Ed.* **1999**, *38*, 3440–3461.

[2] Z. Gao, S. Rohani, J. Gong, J. Wang, *Engineering* **2017**, *3*, 343–353.

[3] A. Llinàs, J. M. Goodman, *Drug Discov. Today* **2008**, *13*, 198–210.

[4] D. B. Amabilino, D. K. Smith, J. W. Steed, *Chem. Soc. Rev.* **2017**, *46*, 2404–2420.

[5] D. Gentili, M. Gazzano, M. Melucci, D. Jones, M. Cavallini, *Chem. Soc. Rev* **2019**, *48*, 2502.

[6] Y. Diao, L. Shaw, Z. Bao, S. C. B. Mannsfeld, *Energy Environ. Sci.* **2014**, *7*, 2145–2159.

[7] Q. Jiang, M. D. Ward, *Chem. Soc. Rev.* **2014**, *43*, 2066–2079.

[8] J. M. Ha, J. H. Wolf, M. A. Hillmyer, M. D. Ward, *J. Am. Chem. Soc.* **2004**, *126*, 3382–3383.

[9] H. Kwon, K. Kim, T. K. An, S. H. Kim, C. E. Park, *J. Ind. Eng. Chem.* **2019**, *75*, 187–193.

[10] G. Giri, S. Park, M. Vosgueritchian, M. M. Shulaker, Z. Bao, *Adv. Mater.* **2014**, *26*, 487–493.

[11] R. Raval, *Faraday Discuss.* **2017**, *204*, 9–33.

[12] Q. Fan, J. Dai, T. Wang, J. Kuttner, G. Hilt, J. M. Gottfried, J. Zhu, *ACS Nano* **2016**, *10*, 3747–3754.

[13] D. Kühne, F. Klappenberger, R. Decker, U. Schlickum, H. Brune, S. Klyatskaya, M. Ruben, J. V Barth, *J. Phys. Chem. C* **2009**, *113*, 17851–17859.

[14] D. G. De Oteyza, E. Barrena, H. Dosch, Y. Wakayama, *Phys. Chem. Chem. Phys.* **2009**, *11*, 8741–8744.

[15] J. Greenwood, T. H. Phan, Y. Fujita, Z. Li, O. Ivasenko, W. Vanderlinden, H. Van Gorp, W. Frederickx, G. Lu, K. Tahara, et al., *ACS Nano* **2015**, *9*, 5520–5535.

[16] L. Verstraete, J. Greenwood, B. E. Hirsch, S. De Feyter, *ACS Nano* **2016**, *10*, 10706–10715.

[17] J. Seibel, L. Verstraete, B. E. Hirsch, A. M. Braganca, S. De Feyter, *J. Am. Chem. Soc.* **2018**, *140*, 11565–11568.

[18] L. Verstraete, J. Smart, B. E. Hirsch, S. De Feyter, *Phys. Chem. Chem. Phys.* **2018**, *20*, 27482–27489.

[19] Y. Hu, A. M. Bragança, L. Verstraete, O. Ivasenko, B. E. Hirsch, K. Tahara, Y. Tobe, S. De Feyter, *Chem. Commun.* **2019**, *55*, 2226–2229.

[20] W. Mamdouh, H. Uji-i, A. Gesquière, S. De Feyter, D. B. Amabilino, M. M. S. Abdel-Mottaleb, J. Veciana, F. C. De Schryver, *Langmuir* **2004**, *20*, 9628–9635.

[21] S. De Feyter, A. Gesquire, K. Wurst, D. B. Amabilino, J. Veciana, F. C. De Schryver, *Angew. Chemie - Int. Ed.* **2001**, *40*, 3217–3220.

[22] L. Verstraete, B. E. Hirsch, J. Greenwood, S. De Feyter, *Chem. Commun.* **2017**, *53*, 4207–4210.

COMMUNICATION

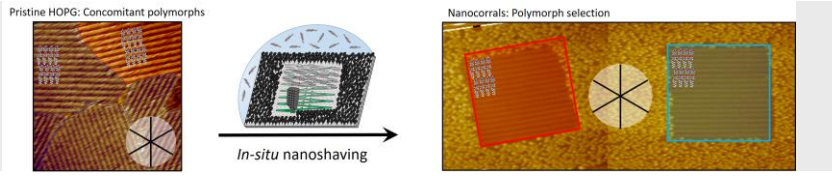

In-situ created nanocorrals can selectively induce the formation of one of two concomitant polymorphs, which otherwise appear simultaneously at the interface of 1-phenyloctane/highly-oriented pyrolytic graphite.

*Johannes Seibel, David B. Amabilino and Steven De Feyter**

Page No. – Page No.

Preferred Formation of Minority Concomitant Polymorphs in 2D Self-Assembly under Lateral Nanoconfinement